50TH EASTERN SNOW CONFERENCE
61ST WESTERN SNOW CONFERENCE
Quebec City 1993

The Permeability of Temperate Snow
Preliminary Links to Microstructure

J.P. HARDY
Geological Sciences Branch
and
D.G. ALBERT
Geophysical Sciences Branch
U.S. Army Cold Regions Research and Engineering Laboratory
72 Lyme Road
Hanover, New Hampshire 03755-1290 U.S.A.

ABSTRACT

The intrinsic permeability of snow is an important parameter controlling meltwater flux through a snowpack and snowpack ventilation. Few measurements have been made on the permeability of seasonal snow covers, particularly in temperate zones where ice layers have an important control on the permeability. The purpose of this research was to correlate field measurements of permeability with physical properties of the snow.

Throughout the 1992–93 winter season, field measurements were made, using an air permeameter, to determine the permeability of different snow types in northern Vermont. Concurrent with the permeability measurements, the physical properties of each stratigraphic layer were measured and samples for microstructural analysis were collected.

Permeability values ranged from 3 to 75×10^{-10} m^2 and agreed with previously published data. No correlation was found between field-measured physical properties and snow permeability. Stereologic parameters for dry snow correlated well with permeability, but for old snow, especially ice layers, the correlation was poor.

INTRODUCTION

The intrinsic permeability of a porous medium defines the ability of a fluid to pass through the medium and is a function of the medium alone, independent of the fluid. The intrinsic permeability of a seasonal snow cover is important because it controls acoustic wave propagation above and through the snow, ventilation and convection in dry snow, and the flow of water through a snowpack. The permeability of snow is difficult to measure for several reasons. Snow metamorphism is constantly occurring and alters the grain and pore shape, porosity, and grain size, which all affect the permeability of the snow. Since snow is a multilayered medium, the determination of a snowpack's permeability is further complicated by layers of varying thickness and differing physical properties. The objective of this report is to present data on the permeability of several snow types, including ice layers, and to correlate these results with measured physical properties of the snow.

There have been few reported measurements on temperate zone seasonal snow covers. Much of the prior work measuring the permeability of snow was done on alpine snow (Bergen, 1968; Conway and Abrahamson, 1984), artificially altered snow (Bender, 1957; Sommerfeld and Rocchio, 1989) or otherwise different snow than found in temperate climates (Chacho and Johnson, 1987). Several permeameters have been described for the measurement of air or kerosene permeability (Kuroiwa, 1968; Shimizu, 1970; Conway and Abrahamson, 1984; Chacho and Johnson, 1987; Sommerfeld and Rocchio, 1989). Reported values for the permeability of several snow types range between 0.4 and 605×10^{-10} m^2 with the majority of the data falling within the range of 5 to 90×10^{-10} m^2.

Previous workers related snow permeability to the density, grain size, and/or age of the snow (Bender, 1957; Ishida and Shimizu, 1958; Shimizu, 1970; Conway and Abrahamson, 1984; Chacho and Johnson, 1987). These correlations showed a large amount of scatter attributable to both experimental error and snow variability. Shimizu (1970) developed an empirical relation for one particular snow type that has since been widely used (Denoth et al., 1979; Sommerfeld and Rocchio, 1989). He found that the permeability, k [m^2], of fine-grained compact snow was related to the specific gravity, ρ [%], and mean grain size, d [m], as

$$k = 0.077 d^2 e^{-7.8\rho}.$$

Shimizu (1970), Martinelli (1971), and Conway and Abrahamson (1984) were not able to find a unique relationship between snow density and permeability. On the other hand, Kuroiwa (1968) observed a logarithmic decrease in permeability when snow samples were artificially compressed to reduce the porosity. Conway and Abrahamson (1984) and Shimizu (1970) observed temporal changes in permeability attributable to differences in grain size and shape due to metamorphism.

No measurements have been published on the low-altitude, temperate-zone seasonal snow where the formation of ice layers is inevitable due to refreezing after midwinter melting or rain-on-snow events. These ice layers dominate and control the permeability of the snowpack, impeding the ventilation by air and the movement of meltwater. In this report, a preliminary analysis of permeability data from northern Vermont is presented for six different snow types, including ice layers. Methods for obtaining values of the permeability of snow, snow cover properties, and microstructural parameters will be presented and their relationships described.

METHODS

The measurements were conducted within the Sleepers River Research Watershed in northern Vermont (44°29′N, 72°09′W, 460 m asl). This region has a mean annual temperature of 6°C and annual precipitation totals that range from 880 to 1270 mm/year, with more than 25% falling as snow (Anderson et al., 1977). Rain-on-snow and midseason melt events occur during the winter season. The test location was a large open field exposed to strong winds from all directions. Throughout the winter, we measured the air permeability of snow samples at this site, made detailed snow pit observations, and collected samples for later microstructural analysis.

Permeability Measurements

Measurements of the permeability of snow were made in the field using an air permeameter described by Chacho and Johnson (1987). The apparatus uses a double-walled cylinder, suggested by Shimizu (1970),

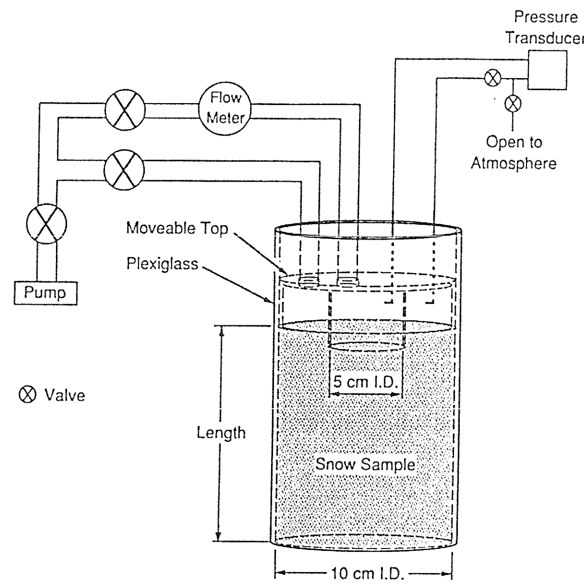

Figure 1. Schematic of air permeameter (after Chacho and Johnson, 1987).

to eliminate effects from cracks or disruption of the snow at the outer edge of the sample (Fig. 1). A Kurz mass flow meter (Model #505) was used to measure flow of air through the sample, with a flow range of 0 to $8.3 \times 10^{-4}\ m^3s^{-1}$ and an accuracy of ± 2% of the measured value. Setra pressure transducers (Model #239) measured the pressure with a range between 0 and 124.6 Pa and an accuracy of ± 0.14%.

To collect a snow sample, a 100-mm-diameter plastic cylinder, with a beveled lower edge, was inserted vertically into the snow layer. The cylinder was isolated by removing snow from around the sample and sliding a flat cutter under the sample. The snow sample was placed on a screen mesh platform and a top, with flexible tubes connected to the pressure transducer and flow meter, was lowered gently onto the snow sample. The top has a 50-mm-diameter inner chamber designed to penetrate 5 mm into the snow surface. The permeability measurements were performed using the inner chamber, where the flow was isolated from the cylinder wall, alleviating the problems associated with disturbed snow on the edge of the sampling cylinder. A vacuum pump was used to draw air through the sample.

Several measurements of pressure at different flow rates were required to adequately determine the snow permeability. Valves controlled air flow and pressure measurements between the inner and outer chambers. The first stage of a measurement was to balance the flow, at the lowest flow possible, by adjusting the flow valves to obtain a zero pressure differential between the inner and the outer chambers. The flow rate through the inner chamber, and the pressure difference between the inner chamber and the atmosphere, were then measured. The next step was to increase the flow rate, balance the flow between the two chambers, and measure the new flow rate and pressure difference between the inner chamber and the atmosphere. These steps were repeated approximately 16 times, giving an output of flow for the entire range of the flow meter.

Darcy's Law and Linear Flow

Laminar flow of a fluid through a porous medium is described by Darcy's law, and takes the form

$$u = -\frac{k}{\mu}\frac{dp}{dx}$$

where u represents the volumetric flow rate per unit area or filter velocity [ms^{-1}], k the intrinsic permeability of the medium [m^2], μ the dynamic viscosity of the fluid [Pa s], and dp/dx the pressure gradient [Pa m^{-1}]. The air permeameter used in this study provided the filter velocity and the pressure gradient across the snow sample.

Darcy's law is valid only for linear flow. To determine the nonlinear flow effects, data from each field test were graphed with filter velocity against the pressure gradient (Fig. 2). As the flow increased, the nonlinear effects were marked by a decrease in the ratio of filter velocity to pressure gradient. This occurred at a filter velocity of 0.056 m s^{-1} in most tests, and is in agreement with Shimizu's (1970) reported filter velocity of up to 0.047 m s^{-1} for laminar flow in snow and up to 0.06 m s^{-1} for medium-sized grains obtained by Bader et al. (1939). Data obtained beyond the linear regime were not used to determine the permeability. A regression line was fit to the linear flow data using the least squares method and the sample permeability was given by the slope of the line times the air viscosity, taken to be 1.78×10^{-5} Pa s at 0°C with an air temperature correction of 5.61×10^{-8} Pa s °C^{-1}. The permeameter was laboratory-tested using glass beads (1-, 2-, and 4-mm diameter) and measured values of permeability compared favorably with theoretical values.

Snowpack Characterization

Each layer within the snowpack was carefully characterized during the snow permeability measurements. Snow temperature, grain size, density, and liquid water content of each stratigraphic layer were measured. Grains were classified according to the International Classification for Seasonal Snow on the Ground (Colbeck et al., 1990).

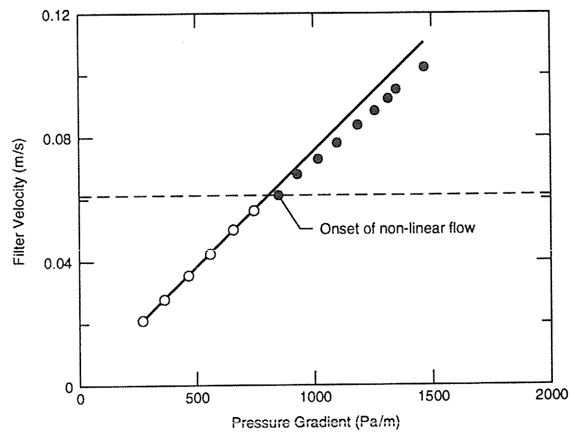

Figure 2. Example of output from permeameter used to determine the onset of nonlinear flow. At a filter velocity of 0.056 m/s, the ratio of filter velocity to pressure gradient begins to decrease, indicating the flow is no longer linear (closed circles). The regression line was determined using the linear flow data only (open circles) and the slope of this line is the permeability with an air viscosity adjustment.

Microstructure Analysis

To ascertain the microstructure of the grains and pores, samples were collected for stereologic analysis. A technique similar to that of Perla (1982) was used to prepare the snow sections. Samples were collected in small plastic containers labeled with the direction to the snow surface. Liquid dimethyl phthalate was used as a pore filler and introduced into the samples at the test site. The samples were then frozen using dry ice and transported to the laboratory cold room. Sample preparation involved microtoming the sample and then letting the snow grains sublimate, leaving a skeleton of dimethyl phthalate showing the pore geometry. Voids created by snow sublimation were filled with black photocopy toner to enhance the contrast between the white "pore space" and the black voids left by the ice structure. A CCD video camera and frame grabber were used to obtain digitized images of the snow samples, which were then classified and analyzed using Image Processing Workbench (IPW) software (Frew, 1990).

Stereologic parameters were computed automatically by passing test lines across the binary image and using equations for counting statistics, as described by Dozier et al. (1987). These equations are valid for either the grain or pore phase. Since air permeability is a function of the air's ability to pass through the pore structure, this stereologic analysis was largely based on results obtained from the pore structure. The three stereologic parameters used in this study, as described by Dozier et al. (1987) were:

Point Density, P_p = number of pixels in all pore profiles/total pixels on section area;

Surface Density, S_v = number of intersections with pore lines/total length of test lines;

Mean Pore Intercept Length (MPIL), L_p, is the mean length of line segments that fall within the pore profile.

P_p is dimensionless, S_v has the units mm^{-1}, and L_p is in mm. The point density of the pore space gives an indication of the overall area occupied by pores and is similar to porosity ø. The surface density is the surface area per unit volume and is a good estimator of mean grain diameter (d_o):

$$d_o = \frac{6}{S_v}(1-\phi).$$

The MPIL is the mean dimension of pore space as averaged over two cartesian directions. Snow density is estimated from the ratio of pixels in the ice profile to the total pixels on the section times the density of ice (917 kg m^{-3}).

RESULTS AND DISCUSSION

Permeability Measurements

A total of 42 tests determined the permeability of several different snow types. Data from 22 tests were chosen for this analysis because of their high quality and range of crystal classes. A description of these crystal classes based on the international classification (Colbeck et al., 1990) is given in Table 1. Figure 3 compares the permeability values obtained for the different snow types. The lowest permeability values (3×10^{-10} m^2) were measured in ice layers, while wet, rounded, melt-freeze grains accounted for the highest values (75×10^{-10} m^2). The lower permeability values for melt-freeze grains in the frozen state compared with those in the wet state may be due to a combination of factors: expansion of water in the pores upon freezing; drainage of water from the wet sample; and/or the evaporation of interstitial water when air was pulled through the sample over a period of tens of minutes. As expected, the new snow par-

Table 1. Morphological description of snow crystals discussed in text. The classification is based on the International Classification of Seasonal Snow on the Ground (Colbeck et al., 1990).

Crystal Classification	Description
1	Precipitation Particles, New Snow
2	Decomposing and Fragmented Precipitation Particles
4	Faceted Crystals (with or without recent rounding)
6	Rounded Wet Grains
8	Ice Masses
9	Surface Deposits and Crusts (including melt-freeze crusts)

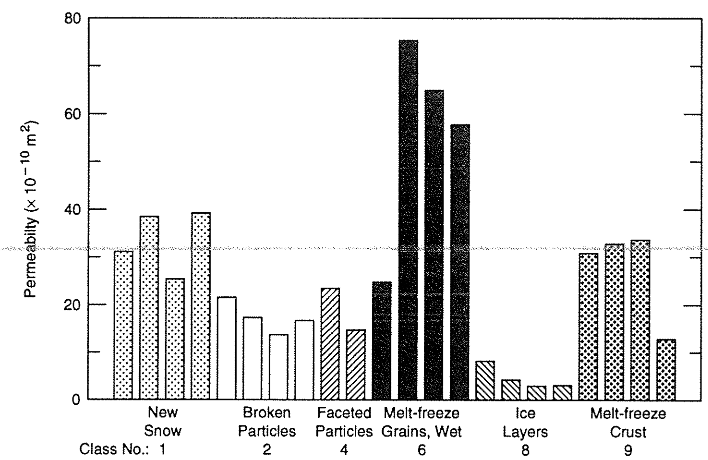

Figure 3. Measured permeability of snow samples from six different crystal classes.

Table 2. The mean, standard deviation (S.D.), and coefficient of variation (c.v.) of permeability data from the different crystal classes (n = 4 for all classes except class 4, where n = 2).

Crystal Class	Mean $\times 10^{-10}m^2$	S.D. $\times 10^{-10}m^2$	c.v. (S.D./mean)100 %
1	34.3	5.7	16.6
2	17.8	2.9	16.3
4	19.5	4.5	23.1
6	55.8	18.8	33.6
8	4.7	2.3	48.7
9	27.8	8.6	30.9

ticles had higher permeability than partly or highly broken particles, which often included a thin surface wind crust. The two permeability values for the mixed grains, where facets were beginning to round, were similar to the broken particles.

Table 2 summarizes the mean, standard deviation and coefficient of variation for the permeability data from the six snow types. The coefficient of variation (c.v.) was used to compare variation between the different snow types and showed the least variability in the new snow and in the wind-packed broken particles. Older snow (including ice layers) showed greater variability in permeability data due, in part, to the effects of metamorphic changes. For example, melt-freeze grains vary in size depending on the number of melt-freeze cycles, and faceted particles will vary with the duration and strength of the temperature gradient. Associated with this higher c.v. for the older snow grains was a higher preliminary estimate of the effect of experimental error on the permeability measurements (~20% compared to ~15% for dry snow).

Relationship to Physical Properties

Other researchers have investigated the relationship between snow porosity and permeability and found that permeability of snow cannot be expressed as a simple function of porosity (i.e., Kuroiwa, 1968). In this study, the porosity ϕ was determined from the measured snow density ρ_s using the relation:

$$\phi = 1 - \rho_s/\rho_i$$

where the density of ice ρ_i is taken to be 917 kg m^{-3} A regression of permeability vs. porosity suggests that porosity alone is a poor indicator of permeability

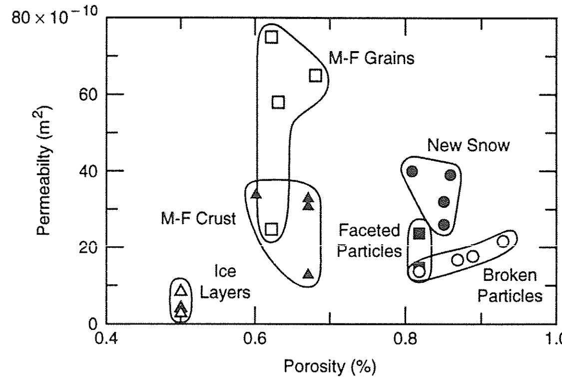

Figure 4. The permeability of snow versus porosity, with data grouped by crystal class.

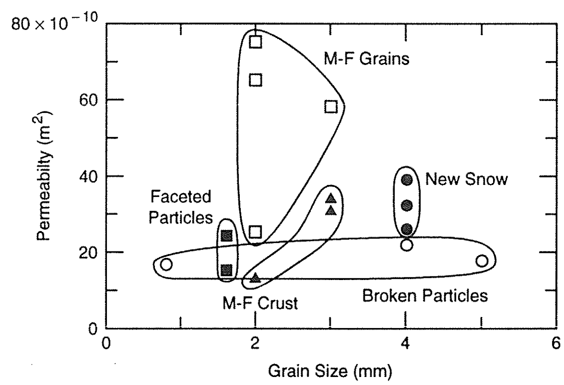

Figure 5. The permeability of snow vs. grain size, with data grouped by crystal class.

($r^2 = 0.013$). When the data were graphed and grouped according to crystal classification (Fig. 4), the porosity, in conjunction with crystal type, helped explain the scatter, but more data are needed to test this tentative relationship. Similarly, the plot of permeability against field-determined grain size (Fig. 5) shows significant scatter even when grouped by crystal class. This comparison of permeability with field-measured porosity and grain size implies that there is no strong relationship between either of these variables alone. Crystal type and shape (and hence geometry of the pore volume) need also to be taken into consideration as possible indicators of the intrinsic permeability of the snow.

Microstructure Analysis

Preliminary microstructure analysis was performed on seven snow samples representing one of each of the six crystal classes described above with two samples representing broken particles. Table 3 summarizes the results of the microstructure analysis and compares it with the porosity, grain size, and

Table 3. Summary of stereologic results of six crystal classes and corresponding snowpit data for porosity (ø), grain size, and snow density (ρ_s). Permeability values are both measured and calculated (in parentheses) using Shimizu's formula and stereologic data. Stereologic parameters are point density (P_p), estimated grain size (d_o), pore dimension (MPIL), and snow density (ρ_s).

			Stereology Measurements				Snow Pit Measurements		
Crystal Class	k $\times 10^{-10}$m^2		P_p —	d_o mm	MPIL mm	ρ_s kg m^{-3}	ø %	Grain Size mm	ρ_s kg m^{-3}
DRY SNOW PORES:									
4	15	(10)	0.63	0.44	0.5	350	0.82	0.8	180
2	18	(14)	0.83	0.26	0.8	160	0.89	2.5	110
2	22	(22)	0.86	0.28	1.1	130	0.93	2.0	70
1	32	(29)	0.87	0.31	1.5	120	0.85	2.0	150
OLD SNOW PORES:									
8	3	(97)	0.45	2.6	1.4	510	0.50	n/a	500*
9	34	(83)	0.48	2.1	1.3	480	0.60	1.5	400
6	58	(82)	0.61	1.3	1.4	360	0.63	1.5	370

* estimated data

density determined from snowpit data. The data were classified into pores in dry snow (new snow, wind-broken snow, and mixed grains) and pores in old snow (melt-freeze grains and ice layers), and sorted by increasing permeability. The microscopic distinction between melt-freeze grains in the wet or frozen state was no longer valid since all samples were frozen prior to filling the pores. As the permeability of the dry snow increased, so did the point density, the MPIL, and the estimated grain size (excepting faceted particles); meanwhile, the snow density decreased. The pore space in the old snow showed a different trend in the stereologic parameters. Only the point density increased with permeability, while the estimated grain size and snow density decreased with a permeability increase and the MPILs showed no trend. The point density was significantly smaller in old snow compared to dry snow and the pore dimension (MPIL) was generally greater in the old snow. The relationship between permeability and the stereologic parameters, P_p and ρ_s, for the class 8 ice layer, fit with the trend of the dry snow, but d_o and MPIL of the ice layer were outliers. Permeability was also calculated using Shimizu's (1970) equation (eq.1) and the stereologic data for d_o and ρ_s. A comparison between the measured and the calculated permeabilities showed reasonable agreement for the dry snow, but the equation failed to predict permeability of the old snow (Table 3).

Microscopic images of new snow and the older melt-freeze crust (Fig. 6) show different pore geometries, yet the permeabilities of the two snow types were very similar (32 and 34 $\times 10^{-10}$ m^2, respectively). The new snow (Fig. 6a) has an open pore structure compared to the old snow (Fig. 6b), where pores are connected pathways. The point density of the old snow was 44% lower than the new snow, while the estimated grain diameter (d_o) of the older snow was almost a factor of 7 larger than the new snow. The MPILs were 13% different and provided the best link, of the measured parameters, between the geometries of the dry and old snow. Neither the field-measured nor the stereologically determined densities explained the similar permeability values. In general, field-measured parameters related poorly with results from stereological methods.

CONCLUSIONS

The air permeability of snow was measured for 22 snow samples representing six different crystal classes. Intrinsic permeability values for samples were in the range of 3 to 75 $\times 10^{-10}$ m^2, and were

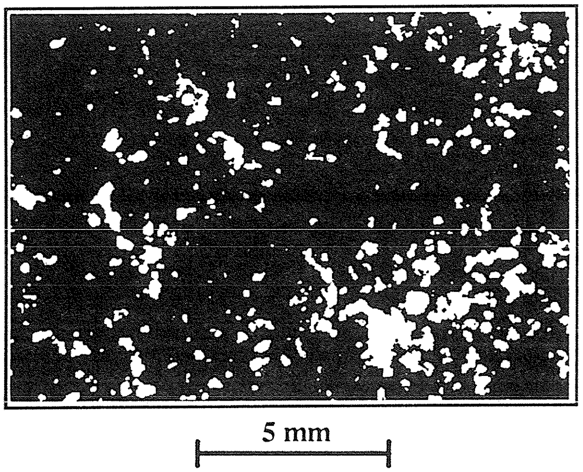

Figure 6a. Microscopic, binary image of new snow (white = snow, black = pore space). This new snow has a density of 120 kg m^{-3}, a porosity of 0.87, an estimated grain size of 0.31 mm, a MPIL of 1.5 mm and a permeability of 32×10^{-10} m^2.

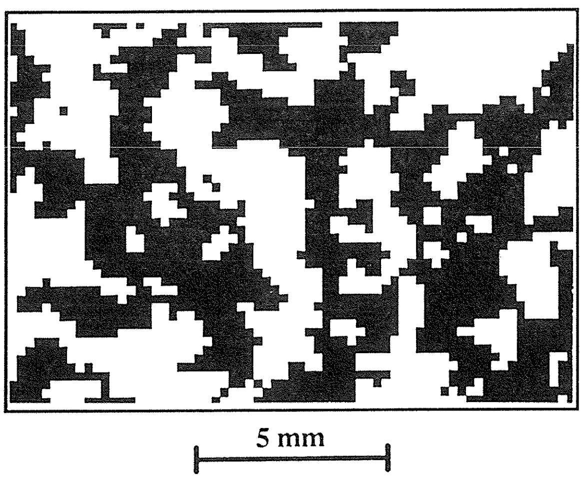

Figure 6b. Microscopic, binary image of a melt-freeze crust (white = snow, black = pore space). This crust has a density of 480 kg/m^3, a porosity of 0.48, an estimated grain size of 2.1 mm, a MPIL of 1.3 mm and a permeability of 34×10^{-10} m^2.

comparable to the majority of data obtained by others on other types of snow. A comparison of these results with snowpit observations suggested that the permeability of snow was not simply related to any easily measured, physical property. The permeability data for older snow were more variable than new snow. Macroscopic data (porosity and grain size) showed no direct relationship to permeability, unless the data were grouped according to crystal class. Even then, field-measured grain sizes were a poor indicator of permeability, due largely to the difficulty of obtaining an accurate measurement in the field.

Measured stereologic parameters for dry snow pores corresponded well with permeability, but the same relationships between the variables did not exist in older snow. Pore profiles of new snow and old snow, with their different geometries and different stereologic parameters, can still yield similar values of permeability. Pore intercept lengths, either the MPIL or a maximum intercept length, may be useful for finding a relationship between permeability and a measured physical parameter.

Future work will include analysis of additional microscopic samples to improve confidence in these results and to investigate potential correlations between the permeability of snow and other physical parameters. Field methods will be refined to better measure the permeability of old snow and in particular, ice layers. Finally, these measurements will be compared with acoustic experiments conducted concurrently to determine the depth integrated permeability of the snowpack.

ACKNOWLEDGEMENTS

This work was funded by the Directorate of Research and Development, U.S. Army Corps of Engineers, Project 4A161102AT24. The authors thank Steve Decato and Mary Albert for some of the snowpack characterization and Bert Davis for help with the snow sample preparation and use of the stereology program. Ed Chacho and Jerry Johnson were very helpful in the initial construction and operation of the permeameter. Finally, we thank the reviewers for their helpful comments.

LITERATURE CITED

Anderson, E.A., H.J. Greenan, R.Z. Whipkey, and C.T. Machell (1977) NOAA-ARS Cooperative Snow Research Project:: Watershed hydro-climatology and data for the water years 1960–1974. USDC and USDA publication, June 1977.

Bader, H., R. Haefeli, E. Bucher, H. Neher, O. Eckel, and C. Thams (1939) Snow and its metamorphism. (Beitrage zur Geologie der schweiz; Lieferung 3, Bern), SIPRE Translation (1954) no. 14, 313 pp.

Bender, J.A. (1957) Air permeability of snow. SIPRE Research Report 37, U.S. Army Corps of Engineers, Snow Ice and Permafrost Research Establishment, November 1957, 27 pp.

Bergen, J.D. (1968) Some measurements of air permeability in a mountain snow cover. Bulletin IAHS, vol. 13, p. 5–13.

Chacho. E.F. Jr. and J.B. Johnson (1987) Air permeability of snow. *EOS Transactions*, American Geophysical Union, **68**: 1271, (abstract only).

Colbeck, S., E. Akitaya, R. Armstrong, H. Gubler, J. Lafeuille, K. Lied, D. McClung, and E. Morris (1990) *The International Classification for Seasonal Snow on the Ground.* Int. Comm. Snow and Ice (ICSI), (available from World Data Center, University of Colorado, Boulder, CO), 23 pp.

Conway, H. and J. Abrahamson (1984) Air permeability as a textural indicator of snow. *Journal of Glaciology*, **30**: 328–333.

Denoth, A., W. Seidenbusch, M. Blumthaler, P. Kirchlechner, W. Ambach, and S. Colbeck (1979) Study of water drainage from columns of snow. U.S. Army Cold Regions Research and Engineering Laboratory, CRREL Report 79-1, 14 pp.

Dozier, J., R. Davis, and R. Perla (1987) *On the objective analysis of snow microstructure, avalanche, formation, movement and effects*. Proceedings of the Davos Symposium, Sept. 1986, IAHS Publication no. 167, p. 49–59.

Frew, J. (1990) The Image Processing Workbench. Ph.D. Dissertation, Department of Geography, University of California, Santa Barbara, CA, July 1990.

Ishida, T. and H. Shimizu (1958) Resistance to air flow through snow layers: Part 1. Low Temperature Science Series A, 1955, no. 14, p. 32–42, SIPRE Translation no. 60, 9 pp.

Kuroiwa, D. (1968) Liquid permeability of snow. General Assembly of Bern, 25 Sept.–7 Oct. 1967, Commission of Snow and Ice, Reports and Discussion, IAHS Publication No. 79, p. 380–391.

Martinelli, M. Jr. (1971) Physical properties of alpine snow as related to weather and avalanche conditions. USDA Forest Service Research Paper RM-64, January 1971, 35 pp.

Perla, R. (1982) Preparation of section planes in snow specimens. *Journal of Glaciology*, **28**(98): 199–204.

Shimizu, H. (1970) Air permeability of deposited snow. Contributions from the Institute of Low Temperature Science, Series A, vol. 22, p. 1–32.

Sommerfeld, R. and J. Rocchio (1989) The Darcy permeability of fine-grained compact snow. Eastern Snow Conference Proceedings, Quebec City, Quebec, 8–9 June 1989, p. 121–128.